Structural Engineering and Mechanics, *Vol. 58, No. 2 (2016) 199-216*
DOI: http://dx.doi.org/10.12989/sem.2016.58.2.199

Vibration behaviors of a damaged bridge under moving vehicular loads

Xinfeng Yin[1a], Yang Liu[*1] and Bo Kong[2b]

[1]School of Civil Engineering and Architecture, Changsha University of Science & Technology, Changsha 410004, Hunan, China
[2]Department of Civil and Environmental Engineering, Louisiana State University, Baton Rouge, Louisiana, 70803, USA

(Received September 14, 2015, Revised December 10, 2015, Accepted December 12, 2015)

Abstract. A large number of bridges were built several decades ago, and most of which have gradually suffered serious deteriorations or damage due to the increasing traffic loads, environmental effects, and inadequate maintenance. However, very few studies were conducted to investigate the vibration behaviors of a damaged bridge under moving vehicles. In this paper, the vibration behaviors of such vehicle-bridge system are investigated in details, in which the effects of the concrete cracks and bridge surface roughness are particularly considered. Specifically, two vehicle models are introduced, i.e., a simplified four degree-of-freedoms (DOFs) vehicle model and a more complex seven DOFs vehicle model, respectively. The bridges are modeled in two types, including a single-span uniform beam and a full scale reinforced concrete high-pier bridge, respectively. The crack zone in the reinforced concrete bridge is considered by a damage function. The bridge and vehicle coupled equations are established by combining the equations of motion of both the bridge and vehicles using the displacement relationship and interaction force relationship at the contact points between the tires and bridge. The numerical simulations and verifications show that the proposed modeling method can rationally simulate the vibration behaviors of the damaged bridge under moving vehicles; the effect of cracks on the impact factors is very small and can be neglected for the bridge with none roughness, however, the effect of cracks on the impact factors is very significant and cannot be neglected for the bridge with roughness.

Keywords: bridges; simulation; dynamic analysis; cracks; surface roughness

1. Introduction

The studies on the bridge vibration under moving vehicles have been conducted extensively and achieved great success during the recent decades. The dynamic performance of bridges can be affected by many factors, such as the vehicle type, vehicle speed, and road surface condition, etc. For a bridge with given structural properties and road surface conditions, the mechanical properties (or dynamic characteristics) of vehicles traveling on the bridge play a very important

∗Corresponding author, Professor, E-mail: Liuyangbridge@163.com
[a]Associate Professor, E-mail: yinxinfeng@163.com
[b]Former Ph.D., E-mail: kongbo_kenny@hotmail.com

http://www.techno-press.org/?journal=sem&subpage=8 ISSN: 1225-4568 (Print), 1598-6217 (Online)

(a)Cracks at beam bottom (b) Cracks at beam web

Fig. 1 The damaged cracks at bottom and web of the beam (Inside of red line is the crack zone)

role in affecting the dynamic response of the structural system. In the literature, many vehicle-bridge interaction models have been proposed. For example, the vehicle was usually simulated as a single degree-of-freedom (DOF) system, two-DOF system (Fryba 1974, Wang *et al*. 1992, Green and Cebon 1997), or a more complex seven DOFs system (Law and Zhu 2005, Deng and Cai 2010a, Zhang and Cai 2012). The bridge was simplified as simply-support beams (Law *et al*. 1997, Law *et al*. 1999, Law *et al*. 2001) or multi-span continuous beams (Zhu and Law 2002, Chan and Ashebo 2006, Yin *et al*. 2010, Yang *et al*. 2013). However, most of these studies were primarily focused on the intact bridge structures, and very few studies examined the behaviors of damaged bridge structures with cracks.

As a matter of fact, a large number of bridges were built several decades ago, and many of which have gradually suffered serious deteriorations or damage due to the increasing traffic loads, environmental effects, material aging, and inadequate maintenance (Czaderski and Maotavalli 2007, AASHTO 2004). For most of the in-service bridges, the cracked zones usually occurred at the bottom or web of the beams, as shown in Fig. 1. These cracks of the concrete may significantly influence vibration performance of the vehicle-bridge system, which deserves a more in-depth investigation.

Some studies have been tentatively conducted on the vehicle-bridge vibration of damaged structures. Lee and Ng (1994) analyzed the dynamic responses of a beam with a single-sided crack under a moving load. Abdel Wahab *et al*. (1999) used a damage function to describe the damage pattern of reinforced concrete beams with three parameters, i.e., the length of damaged zone, the magnitude of damage, and the variation of the Young's modulus of material. Mahmoud and Abou Zaid (2002) studied the dynamic responses of simply supported beams with transverse cracks subjected to a moving mass. Law and Zhu (2004) presented a method to assess the condition and load-carrying capacity of a damaged simply supported beam. Ariaei *et al*. (2009) demonstrated the differences between the displacement responses of the intact beam and cracked beam. Nguyen and Tran (2010) studied a cracked bridge subject to a moving vehicular load by analyzing the time history of deflections from a vehicle-bridge system. Khoa (2013) studied the open and breathing crack detections of a beam subjected to a simple moving vehicle. As can be noted, some simplified assumptions were made in all above studies. The complicated bridge structures, vehicles, and crack mechanisms were simplified into the simply supported beams, moving loads, and simple crack models. In addition, one of the most important key factors i.e., the impact factor, was almost not fully investigated during the above analysis of bridge-vehicle interaction responses. The neglect of these two perspectives may results in an incomprehensive understanding of the bridge vibration under moving vehicles.

This study is mainly focused to study the dynamic responses of a high-pier bridge under moving vehicular loads, where the effects of the concrete cracks and bridge surface roughness are considered. Specifically, two vehicle models, (i.e., a four DOFs vehicle model and a seven DOFs vehicle model), and two bridge models, (i.e., a single-span uniform beam and a real reinforced concrete high-pier bridge), are respectively introduced. The crack zone in the reinforced concrete bridge is modeled as a damage function. The bridge-vehicle coupled equations are established by combining the equations of motion of both the bridge and vehicles, together with considering the displacement and interaction force relationships at the contact points between the bridge and tires. The numerical simulations and verifications demonstrate that the proposed methodology can rationally simulate the vibration behaviors of the damaged bridge under moving vehicles.

2. Model of vehicle-bridge coupled system

2.1 Vehicular load model

The three-dimensional mathematical model for a vehicle is shown in Fig. 2. The vehicular body is assigned three DOFs, each corresponding to the vertical displacement (y_t), pitch rotation about the transverse axis (θ_t), and roll rotation about the longitudinal axis (ϕ_t). Each wheel/axle has two degrees of freedom in the vertical and roll directions ($\mathrm{y_a}^1, \mathrm{y_a}^2, \phi_a^{\ 1}, \phi_a^{\ 2}$), respectively. Thus, the total number of the independent degrees of freedom is seven. The equations of motion of the vehicle are derived using the Lagrange's formulation as follows.

The vertical displacements of the suspension springs of the vehicle can be written as

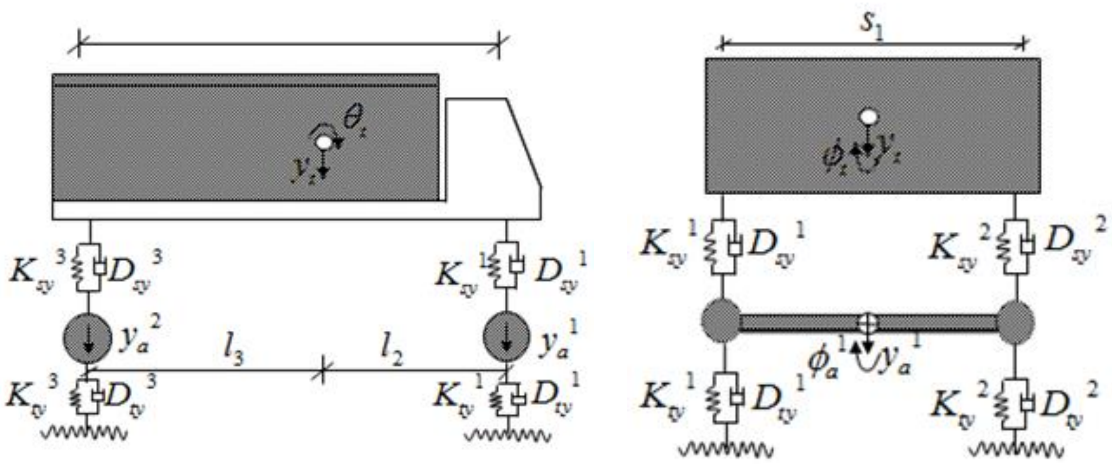

(a) Elevation View (b) Cross-sectional View

Fig. 2 Idealization of two-axle vehicle: (a) Elevation view; (b) Cross-sectional view

$$U_{sy}{}^{1} = (y_t - y_a{}^{1}) + (s_1/2)(\phi_t - \phi_a{}^{1}) + l_2\theta_t \tag{1}$$

$$U_{sy}{}^{2} = (y_t - y_a{}^{1}) - (s_1/2)(\phi_t - \phi_a{}^{1}) + l_2\theta_t \tag{2}$$

$$U_{sy}{}^{3} = (y_t - y_a{}^{2}) + (s_2/2)(\phi_t - \phi_a{}^{2}) - l_3\theta_t \tag{3}$$

$$U_{sy}{}^{4} = (y_t - y_a{}^{2}) - (s_2/2)(\phi_t - \phi_a{}^{2}) - l_3\theta_t \tag{4}$$

where $U_{sy}{}^{i}$ (i=1, 2, 3, and 4) is the vertical displacements of axles; l_2 is the distance between the front axle and the center of the vehicle; l_3 is the distance between the rear axle and the center of the vehicle; and s_1 and s_2 are the distance between two tires at each of the front and rear axles, respectively.

The vertical elastic and damping forces of the i^{th} (i=1, 2, 3, and 4) vehicle suspension can be written as

$$F_{sy}{}^{i} = K_{sy}{}^{i}U_{sy}{}^{i} \tag{5}$$

$$F^{i}_{dsy} = D^{i}_{sy}\dot{U}^{i}_{sy} \tag{6}$$

where $U_{sy}{}^{i}$ (i=1, 2, 3, and 4) is the vertical displacements of each tire and can be expressed as

$$U_{tyx}{}^{1} = y_a{}^{1} + (s_1/2)\phi_a{}^{1} - [-r(x)^{1}] - y^{1}_{b\_contact} \tag{7}$$

$$U_{tyx}{}^{2} = y_a{}^{1} - (s_1/2)\phi_a{}^{1} - [-r(x)^{2}] - y^{2}_{b\_contact} \tag{8}$$

$$U_{tyx}{}^{3} = y_a{}^{2} + (s_2/2)\phi_a{}^{2} - [-r(x)^{3}] - y^{3}_{b\_contact} \tag{9}$$

$$U_{tyx}{}^{4} = y_a{}^{2} - (s_2/2)\phi_a{}^{2} - [-r(x)^{4}] - y^{4}_{b\_contact} \tag{10}$$

where $r(x)$ represents the vertical bridge surface roughness at x location of the i^{th} (i=1, 2, 3, and 4) tire contact position; $y^{i}_{b\_contact}$ represents the bridge dynamic vertical deflection at x location of the i^{th} (i=1, 2, 3, and 4) tire contact position with bridge.

The vertical bridge-vehicle interaction forces acting at the bridge surface can be written as

$$F_{ty}{}^{i} = K_{ty}{}^{i}U_{ty}{}^{i} \tag{11}$$

$$F^{i}_{dty} = D^{i}_{ty}\dot{U}^{i}_{ty} \tag{12}$$

Therefore, the equations of motion of the full-scale vehicle can be obtained from the Lagrangian formulation and expressed as

$$m_t\ddot{y}_y + (F^1_{sy} + F^2_{sy} + F^3_{sy} + F^4_{sy}) + (F^1_{dsy} + F^2_{dsy} + F^3_{dsy} + F^4_{dsy}) = m_t g \tag{13}$$

$$\begin{gathered} I_{xt}\ddot{\phi}_t + (s_1/2)(F^1_{sy} - F^2_{sy}) + (s_2/2)(F^3_{sy} - F^4_{sy}) + \\ (s_1/2)(F^1_{dsy} - F^2_{dsy}) + (s_2/2)(F^3_{dsy} - F^4_{dsy}) = 0 \end{gathered} \tag{14}$$

$$I_{zt}\ddot{\theta}_t + l_2(F_{sy}^1 + F_{sy}^2) - l_3(F_{sy}^3 + F_{sy}^4) + l_2(F_{dsy}^1 + F_{dsy}^2) - l_3(F_{sy}^3 + F_{sy}^4) = 0 \tag{15}$$

$$m_{a1}\ddot{y}_a^1 - (F_{sy}^1 + F_{sy}^2) + (F_{ty}^1 + F_{ty}^2) - (F_{dsy}^1 + F_{dsy}^2) + (F_{dst}^1 + F_{dst}^2) = m_{a1}g \tag{16}$$

$$\begin{aligned} &I_{xa1}\ddot{\phi}_a^1 - (s_1/2)(F_{sy}^1 - F_{sy}^2) + (s_1/2)(F_{ty}^1 - F_{ty}^2) - \\ &(s_1/2)(F_{dsy}^1 - F_{sdy}^2) + (s_1/2)(F_{dst}^1 - F_{dst}^2) = 0 \end{aligned} \tag{17}$$

$$m_{a2}\ddot{y}_a^2 - (F_{sy}^3 + F_{sy}^4) + (F_{ty}^3 + F_{ty}^4) - (F_{dsy}^3 + F_{dsy}^4) + (F_{dty}^3 + F_{dty}^4) = m_{a2}g \tag{18}$$

$$\begin{aligned} &I_{xa2}\ddot{\phi}_a^2 - (s_2/2)(F_{sy}^3 - F_{sy}^4) + (s_2/2)(F_{ty}^3 - F_{ty}^4) - \\ &(s_2/2)(F_{dsy}^3 - F_{sdy}^4) + (s_2/2)(F_{dty}^3 - F_{dty}^4) = 0 \end{aligned} \tag{19}$$

Eqs. (13)-(19) can be rewritten in a matrix form as

$$[M_v]\{\ddot{y}_v\} + [C_v]\{\dot{y}_v\} + [K_v]\{y_v\} = \{F_G\} + \{F_{v-b}\} \tag{20}$$

Where $[M_v]$, $[C_v]$, $[K_v]$=mass, damping, and stiffness matrices of the vehicle, respectively; $\{y_v\}$= vector of the vertical displacements of the vehicle; $\{F_G\}$=gravity force vector of the vehicle; and $\{F_{v\text{-}b}\}$=vector of the wheel-road contact forces acting on the vehicle.

2.2 Equations of motion of bridge model

The equation of motion of a bridge can be written as

$$[M_b]\{\ddot{U}_b\} + [C_b]\{\dot{U}_b\} + [K_b]\{U_b\} = \{F_{b\text{-}v}\} \tag{21}$$

Where $[M_b]$, $[C_b]$, and $[K_b]$ are the mass, damping, and stiffness matrices of the bridge, respectively; $\{U_b\}$ is the displacement vector for all DOFs of the bridge; $\{\dot{U}_b\}$ and $\{\ddot{U}_b\}$ are the first and second derivative of $\{U_b\}$ with respect to time, respectively; and $\{F_{v\text{-}b}\}$ is a vector containing all external forces acting on the bridge.

2.3 Assembling the vehicle-bridge coupled system

Using the displacement relationship and the interaction force relationship at the contact points between bridge and tires, the vehicle-bridge coupled system can be established by combining the equations of motion of both the bridge and vehicle, as shown below

$$\begin{bmatrix} M_b & \\ & M_v \end{bmatrix}\begin{Bmatrix} \ddot{y}_b \\ \ddot{y}_v \end{Bmatrix} + \begin{bmatrix} C_b + C_{b-b} & C_{b-v} \\ C_{v-b} & C_v \end{bmatrix}\begin{Bmatrix} \dot{y}_b \\ \dot{y}_v \end{Bmatrix} + \begin{bmatrix} K_b + K_{b-b} & K_{b-v} \\ K_{v-b} & K_v \end{bmatrix}\begin{Bmatrix} y_b \\ y_v \end{Bmatrix} = \begin{Bmatrix} F_{b-r} \\ F_{b-r} + F_G \end{Bmatrix} \tag{22}$$

where $C_{b\text{-}b}$, $C_{b\text{-}v}$, $C_{v\text{-}b}$, $K_{b\text{-}b}$, $K_{b\text{-}v}$, $K_{v\text{-}b}$, and $F_{b\text{-}r}$ are related to the contact forces at the interface of the wheel and bridge. Since the positions of the contact points, as well as the contact forces, change with the vehicle moving along the bridge, all these sever terms are time-dependent and varied with different vehicle positions on the bridge.

To simplify the bridge model and save computation effort, the modal superposition technique method can be used; the displacement vector of the bridge $\{y_b\}$ in Eq. (22) can be expressed as:

$$\{y_b\} = \left[\{\Phi_1\} \quad \{\Phi_2\}\ldots\{\Phi_n\}\right]\{\xi_1 \quad \xi_2\cdots\xi_n\}^T = [\Phi_b]\{\xi_b\} \tag{23}$$

where n is the total number of modes used for the bridge; $\{\Phi_i\}$ and ξ_i are the i^{th} (i=1..n) mode shape of the bridge and the i^{th} generalized modal coordinate, respectively. Each mode shape is normalized such that $\{\Phi_i\}^T[M_b]\{\Phi_i\}=1$ and $\{\Phi_i\}^T[K_b]\{\Phi_i\}=\omega_i^2$.

Assuming $[C_b]$ in Eq. (22) equal to $2\omega_i\eta_i[M_b]$, where η_i is the percentage of the critical damping for the i^{th} mode of the bridge, Eq. (22) can be simplified as

$$\begin{aligned}\begin{bmatrix} I & \\ & M_v \end{bmatrix}\begin{Bmatrix}\ddot{\xi}_b \\ \ddot{y}_v\end{Bmatrix} + \begin{bmatrix} 2\omega_i\eta_i I + \Phi_b^T C_{b-b}\Phi_b & \Phi_b^T C_{b-v} \\ C_{v-b}\Phi_b & C_v \end{bmatrix}\begin{Bmatrix}\dot{\xi}_b \\ \dot{y}_v\end{Bmatrix} \\ + \begin{bmatrix} \omega_i^2 I + \Phi_b^T K_{b-b}\Phi_b & \Phi_b^T K_{b-v} \\ K_{v-b}\Phi_b & K_v \end{bmatrix}\begin{Bmatrix}\xi_b \\ y_v\end{Bmatrix} = \begin{Bmatrix}\Phi_b^T F_{b-r} \\ F_{v-r} + F_G\end{Bmatrix}\end{aligned} \tag{24}$$

The vehicle-bridge coupled system in Eq. (24) contains only the modal properties of the bridge and the physical parameters of the vehicles. As a result, the complexity of solving the vehicle-bridge coupling equations is greatly reduced. Eq. (24) is solved by the Newmark-β method in time domain.

2.4 Damage functions of the reinforced concrete bridge

When dealing with cracks in the concrete bridge, Abdel Wahab *et al*. (1999) used a damage function to describe the damage pattern of reinforced concrete beams with three parameters, i.e. the length of damaged zone, the magnitude of damage, and the variation of the Young's modulus of material from the center to the ends of the damaged zone. Law and Zhu (2004) verified the accuracy of this proposed damage function with the dynamic tests on a simply supported reinforced concrete bridge deck. In the present paper, such same damage function was used to study the effects of cracks on the vehicle-bridge coupled vibration.

Based on the results in Abdel Wahab *et al*. (1999), the damage in a reinforced concrete beam is considered as a reduction in the Young's modulus of material with the following function

$$\begin{gathered} EI(x) = E_0 I(1-\alpha\cos^2(\frac{\pi}{2}(\frac{|x-l_c|}{\beta L/2})^m)) \\ (l_c - \beta L/2 < x < l_c + \beta L/2) \end{gathered} \tag{25}$$

Where α, β, and m are the damage parameters. l_c denotes the mid-point of the damage zone from the left support of the beam. β characterizes the length of the damaged zone and the value is in the range between 0.0 and 1.0. α characterizes the magnitude of the damage and the value is between 0.0 and 1.0. The beam is intact when α equals to 0.0; and the bending stiffness of the damage zone is zero when α equals to 1.0. m characterizes the variation of the Young's modulus from the center to the two ends of the damage zone. If m is larger than 1, a flat damage pattern is produced; otherwise a steep pattern is generated. E_0 is the modulus of the intact beam. A sketch of the proposed function is shown in Fig. 3. According to the above definition, the stiffness of an element with an open crack zone can then be expressed as

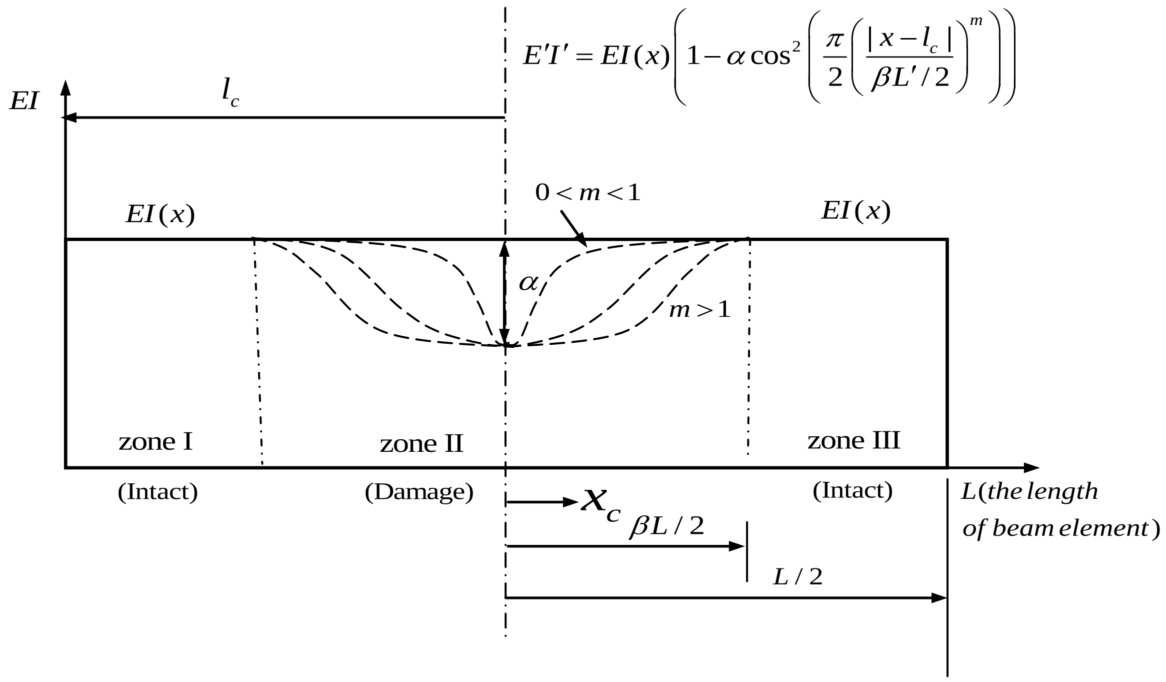

Fig. 3 A sketch of the damage function

$$k_{bij} = E_0 I\left[\int_0^{l_c-\beta L/2}\phi_i''(x)\phi_j''(x)dx + \int_{l_c-\beta L/2}^{l_c+\beta L/2}(1-\alpha\cos^2(\frac{\pi}{2}(\frac{|x-l_c|}{\beta L/2})^m))\phi_i''(x)\phi_j''(x)dx + \int_{l_c+\beta L/2}^{L}\phi_i''(x)\phi_j''(x)dx\right]/M_i(i,j=1,2,...,n) \tag{26}$$

2.5 Bridge surface condition

The bridge surface condition is an important factor that affects the dynamic responses of both the bridge and vehicles. The bridge surface profile is usually assumed to be a zero-mean stationary Gaussian random process and can be generated through an inverse Fourier transformation based on a power spectral density (PSD) function (Yin *et al*. 2011) as

$$r(x) = \sum_{k=1}^{N}\sqrt{2\varphi(n_k)\Delta n}\cos(2\pi n_k x + \theta_k) \tag{27}$$

where θ_k is the random phase angle uniformly distributed from 0 to 2π; $\varphi()$ is the PSD function for the elevation of the bridge surface; and n_k is the wave number. In the present study, the following PSD function (Yin *et al*. 2011) has been used

$$\varphi(n) = \varphi(n_0)(\frac{n}{n_0})^{-2} \qquad (n_1 < n < n_2) \tag{28}$$

where n is the spatial frequency; n_0 is the discontinuity frequency of $1/2\pi$; $\varphi(n_0)$ is the roughness coefficient which is determined based on the road condition; and n_1 and n_2 are the lower and upper

Table 1 Values of $\varphi(n_0)$ for road roughness classifications

Classifications	Ranges of $\varphi(n_0)$
Very good	2×10^{-6} to 8×10^{-6}
Average	8×10^{-6} to 32×10^{-6}
Poor	32×10^{-6} to 128×10^{-6}
Very poor	512×10^{-6} to 2048×10^{-6}

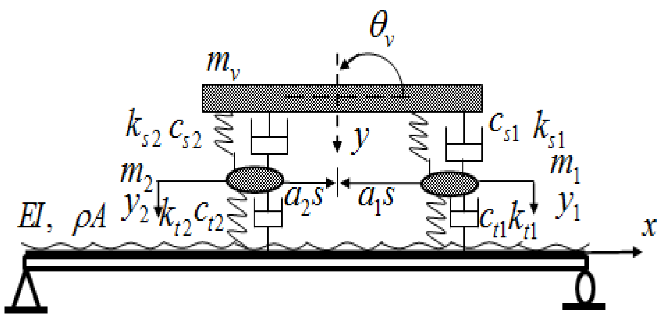

Fig. 4 The simply supported beam model subjected to a moving vehicle

cut-off frequencies, respectively. The International Organization for Standardization (1995) has proposed a road roughness classification index from A (very good) to H (very poor) according to different values of $\varphi(n_0)$ shown in Table 1.

2.6 Impact factor

As discussed in the above section, the impact factor is generally treated as a key factor to reflect the dynamic effect of moving vehicles. This factor is usually served to provide guidelines for bridge design. However, the impact factors of the damaged bridge were not studied and thus not included in the current design codes.

In this study, the impact factor is defined as follows

$$IM = \frac{R_d(x) - R_s(x)}{R_s(x)} \tag{29}$$

where $F_d(x)$ and $R_s(x)$ are the maximum dynamic and static responses of the bridge at location x, respectively.

3. Numerical examples

3.1 Case one-a uniform single-span cracked beam

To verify the proposed method, a comparison is made with the prediction from Law and Zhu (2004) on the normalized mid-span deflection of the beam with a moving vehicle model. Fig. 4 shows the vehicle-bridge coupled system. The parameters of the simply supported beam are L=30 m, EI=2.5x10^{10}Nm^2, ρA=5000 kg/m. The parameters of the crack zone are α=0.5, β=0.5, m=2.0, and l_c=0.5. The characteristics of the 4 DOFs vehicle model are m_v=17735 kg, m_1=1500 kg, m_2=1000 kg, S=4.27 m, a_1=0.519, a_2=0.481, k_{s1}=2.47×10^6 Nm^{-1}, k_{s2}=4.23×10^6 Nm^{-1}, k_{t1}=3.74×10^6 Nm^{-1}, k_{t2}=4.60×10^6 Nm^{-1}, c_{s1}=3.00×10^4 Nm^{-1}, c_{s2}=4.00×10^4 Nm^{-1}, c_{t1}=3.90×10^3 Nm^{-1}, c_{t2}=4.30×10^3 Nm^{-1}.

3.1.1 Comparison of the beam deflections

Fig. 5 shows the comparison of the beam normalized deflections, which is calculated by the dynamic deflection responses divided by the static deflections. The later value is calculated when the static vehicle weight is exerted at the mid-span of the beam. It can be observed that the proposed approach gives the same results as that from Law and Zhu (2004) for both the cracked and intact cases under vehicle with either 15 m/s or 30 m/s. Therefore, the proposed method is valid. In addition, the crack at the mid-span can significantly affect the deflections of the beam under a moving vehicle. For example, the maximum normalized deflections at mid-span increase approximately twice when intact beam is cracked.

3.1.2 Effect of road surface roughness

The bridge surface condition is an important factor that affects the dynamic responses of intact bridges based on the studies in Yin *et al*. (2011), Deng and Cai (2010b, 2011). However, in Law and Zhu (2004), the effect of surface condition on the dynamic responses of damaged beam was not studied. In this section, such effects of bridge roughness on damaged bridges are discussed. Fig. 6 shows the comparison results of beam normalized deflections under three conditions, including None roughness, Average, and Poor. The two vehicle speed cases are also included. Based on the simulation results, the normalized deflections increase when the bridge roughness condition changes from None roughness to Poor. For example, the maximum normalized deflections at the mid-span change from 1.92 to 2.51 for None and Poor roughness conditions. In

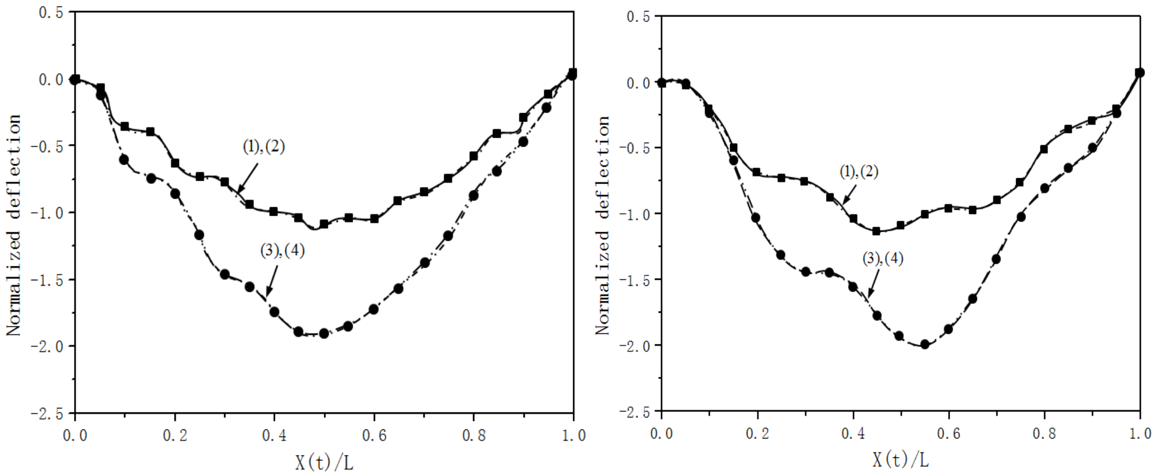

(a) V=15 m/s (b) V=30 m/s

Fig. 5 The comparsion of the beam deflection with exsiting methods[(1)—Law and Zhu (2004) (intact); (2)- - ▪ - - Proposed approach (intact); (3)_ . _ Law and Zhu (2004) (cracked); (4)- - • - - Proposed approach (cracked)]

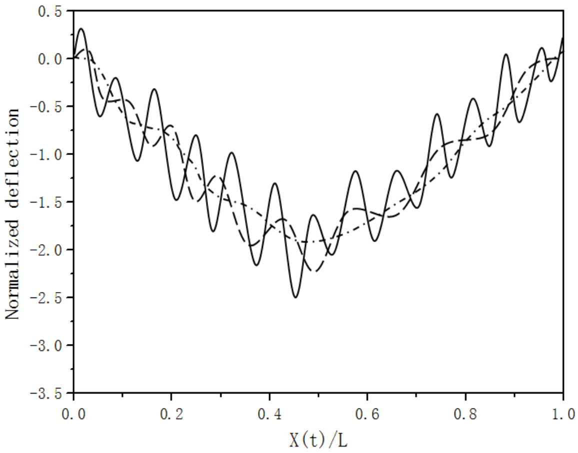

(a) V=15 m/s

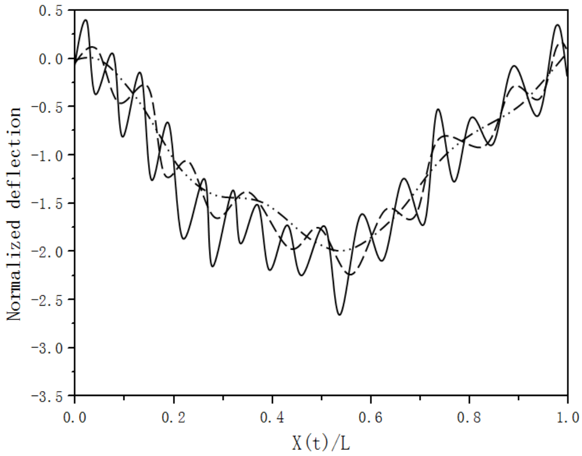

(b) V=30 m/s

Fig. 6 The comparison of the beam displacements under bridge surface roughness (__ . . __None roughness; -----Average ; _____Poor)

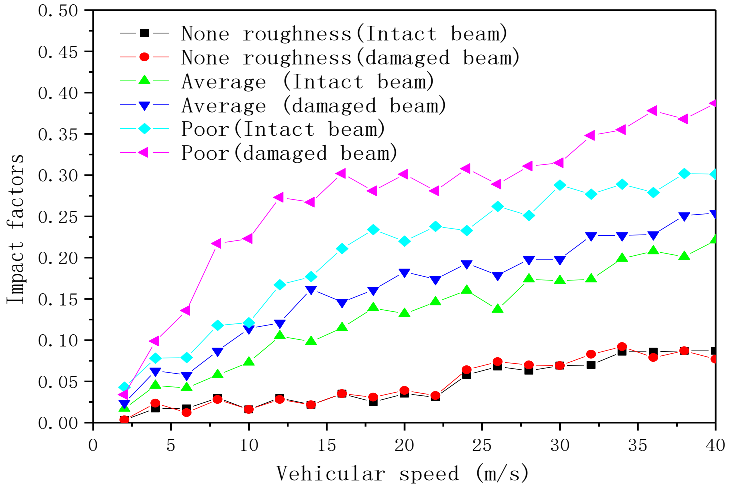

Fig. 7 Impact factors of damaged beam

this sense, it can be stated that the bridge surface condition has a great influence on the vibration of damaged bridges.

3.1.3 Impact factors of cracked beam

The impact factor of damaged bridge can be calculated as the changes of deflections between the static and dynamic conditions as described in Eq. (29). However, the cracks usually can simultaneously increase the beam deflections under either the static or dynamic condition. Therefore, the effect of cracks on impact factors of damaged beams cannot be directly obtained. This uncertainty will be clarified in this section, where three roughness conditions and vehicle speeds from 2.5 m/s to 40m/s are varied in the intact and damaged beam cases.

As shown in Fig. 7, the effect of cracks on the impact factors is very small and can be neglected for bridge surface with none roughness condition. For the Average and Poor surface roughness conditions, however, the effect of cracks become significant. Taking one of the most obvious Poor surface roughness condition for an example, the impact factors are as large as 0.220 and 0.301, respectively, corresponding to the intact beam and damaged beam for the vehicle traveling with 20 m/s. In addition, another two important trends are also shown in Fig. 7. The impact factors of both intact and damaged beams are varied with the vehicular speeds and bridge surface roughness conditions. The higher vehicle speed and the poorer roughness surface induce the larger impact factors.

3.2 Case two-a reinforced concrete high-pier bridge

A typical high-pier bridge, located at the Luping town in Hunan province of China, is discussed as a case to examine the proposed method and the corresponding bridge vibration behaviors. The bridge is a seven-span and straight continuous beam bridge with each span 40 m long and 12 m wide. The bridge elevation view and its cross section view are shown in Fig. 8. The vertical road roughness of the contact points corresponding to the vehicular wheels acting on the road surface was measured and shown in Fig. 9. The time histories of the vertical displacements of mid-span for the fourth span were measured independently using the dynamic measurement system. Using the ambient vibration method and the given crack parameters, the damage function can be used to modify the he stiffness of an element in the bridge finite element model, and bridge modal tests were performed to update the finite element model of Luping Bridge as shown in Fig. 10. More details of the test setups and model updating process can be referred to Yin *et al*. (2011). For the convenience of reviewer, the relevant parameters of the full-scale vehicle are shown in Table 2. It should be noted that only the dimensions, axle loads, and total weight of the vehicle were measured and can be treated as reliable information. The values of suspension stiffness and

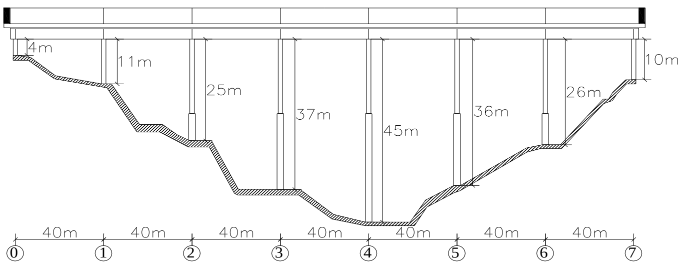

(a) elevation view

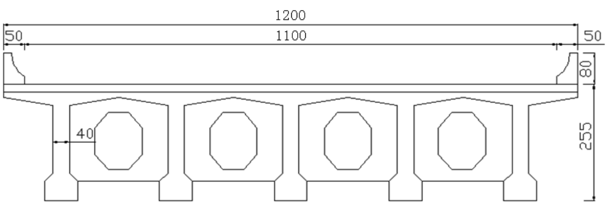

(b) cross section view

Fig. 8 Luping Bridge: (a) elevation view, and (b) cross section view

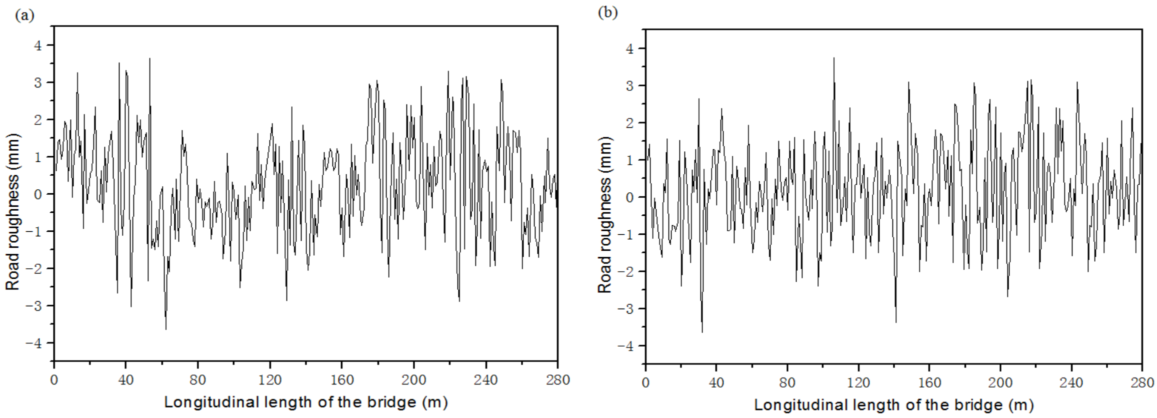

(a) Roughness of the left wheel (b) Roughness of the right wheel

Fig. 9 Road roughness of the bridge: (a) Roughness of the left wheel and (b) Roughness of the right wheel

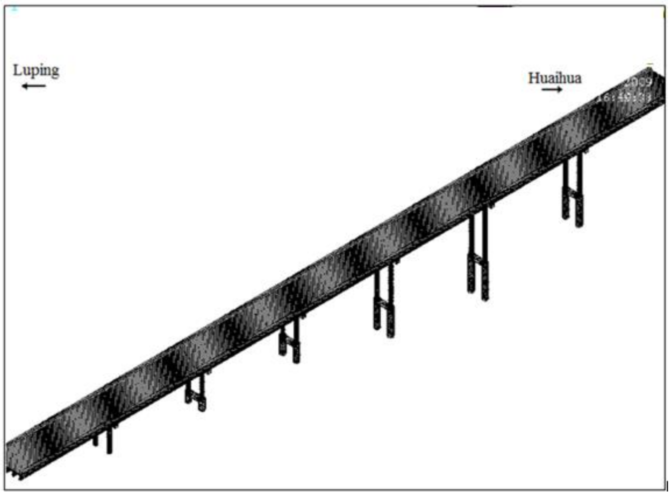

Fig. 10 FE model of Luping bridge

damping, however, might not be exactly the same as that from the actual trucks, which may results in some errors. This inaccuracy can be generally accepted based on previous studies (Yin *et al*. 2011, Yang *et al*. 2004) and will not affect the discussions and conclusions in the present study.

3.2.1 Comparison of vertical displacement

Fig. 11 shows the comparison of the simulations and measurements of displacements at the mid-span of the fourth span. The vehicle was traveling along the center of bridge with two types of constant speeds. It can be seen that the general trend of the simulated and measured mid-span response of the bridge matches very well, thus, the proposed method can appropriately simulate the bridge-vehicle coupled vibration behavior. Some minor differences are observed which may be explained with two reasons. Firstly, the bridge model and the vehicle model may be different from the real bridge and truck used in the test. Secondly, the human errors in controlling the truck locations would affect the accuracy of the measured data.

Table 2 The parameters of the full-scale vehicle

Vehicle Parameter	Value
Mass of truck body m_t	24808 kg
Pitching moment of inertia of truck body I_{zt}	172,160 kg.m^2
Rolling moment of inertia of truck body I_{xa1},I_{xa2}	31,496 kg.m^2
Mass of truck front axle m_{a1}	724kg
Mass of truck rear axle m_{a2}	800kg
Suspension spring vertical stiffness of the first axle K_{sy}^1, K_{sy}^2	242604 (N/m)
Suspension vertical damper of the first axle D_{sy}^1, D_{sy}^2	2190 (N.s/m)
Suspension spring vertical stiffness of the second axle K_{sy}^3, K_{sy}^4	1903172(N/m)
Suspension damper coefficient of the second axle D_{sy}^3, D_{sy}^4	7982 (N.s/m)
Stiffness of the tires for front axle	1,972,900 (N/m)
Stiffness of the tires for rear axle	4,735,000 (N/m)
Distance between the front and the center of the truck l_1	3.73m
Distance between the rear axle and the center of the truck l_2	1.12m
Distance between the right and left axles s_1	2.40m

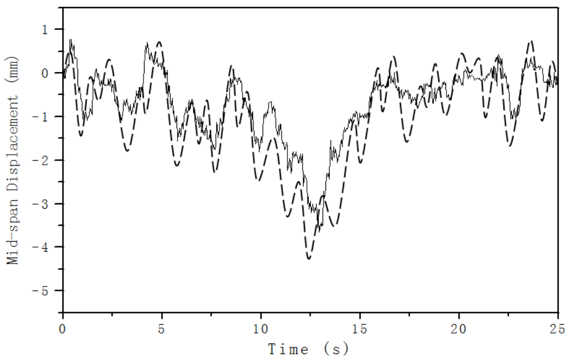

(a) Vehicle speed=40 km/h

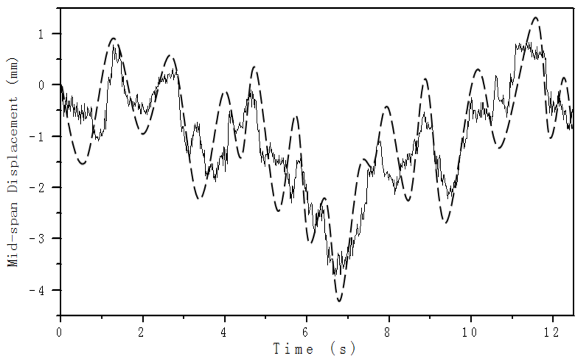

(b) Vehicle speed=80 km/h

Fig. 11 Comparison of simulated and measured responses of intact beam (—— measured; ------ simulated)

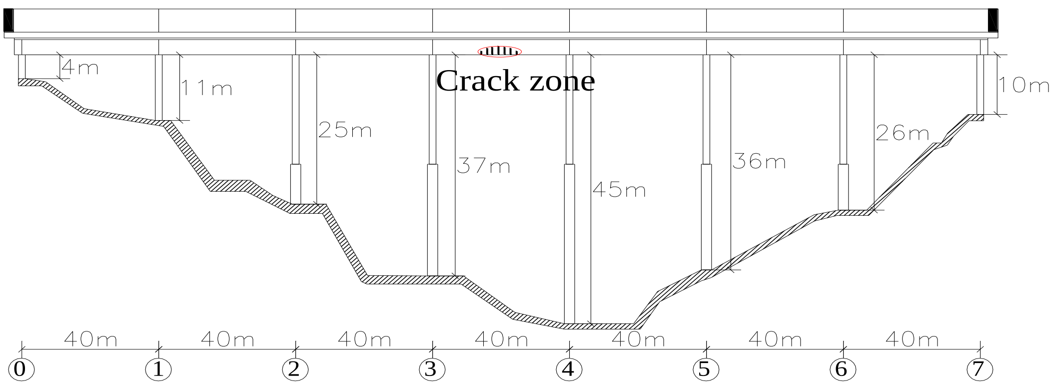

Fig. 12 A cracked zone at location of mid-span of the fourth span

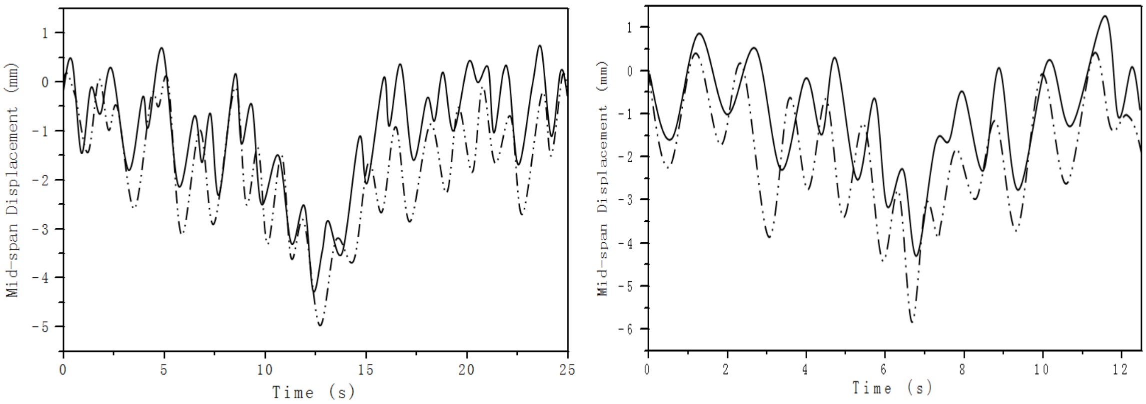

(a) Vehicle speed=40 km/h (b) Vehicle speed=80 km/h

Fig. 13 The comparison of the beam displacements with cracked and intact beams (——— Intact beam; — . . — Cracked beam with a cracked zone)

3.2.2 Comparison of the beams deflections

The effects of the crack zone on the deflection of bridge were studied in this section, where the damaged zone was assumed at location of mid-span of the fourth span, as shown in Fig. 12, with the parameters of α=0.5, β=0.25, m=2.0, and l_c=1/3. It can be seen from Fig. 13 that the effects of crack zone on the vertical deflections at the mid-span of the fourth span for the real bridge are significant. For example, for the vehicle speed with 40 km/h, the maximal vertical deflections increase from 4.3 mm for intact beam to 5.0 mm for the damaged beam. In this sense, the crack zone is a key factor to the bridge vibration for such a full scale high-pier bridge.

3.2.3 Effect of the crack zone number

Three damaged zones were considered at three locations of mid-span of the third span, fourth span, and fifth span. Each damaged crack zone has the same parameters of α=0.5, β=0.25, m=2.0, and l_c=1/3. The effects of the three crack zones on the deflections at the mid-span of the fourth span for the bridge were shown in Fig. 14. It can be seen that effects of the beam deflections increase as the number of crack zones increases, and the maximal deflection for the beam with three crack zones is 1.40 times of that for the beam with one crack zone. Therefore, the number of crack zone is also an important factor to the vibration of cracked bridge.

In addition, for the most in-serviced bridge under the action of moving vehicles, the cracked zones may occur at the bottom and web of the beam, as discussed in Fig. 1. For the vehicles moving on the cracked beam, the length and height of the crack would be enlarged. For a case when the small cracked zone of α=0.5, β=0.25, m=2.0, and l_c=1/3 is developed to the large cracked zone of α=0.58, β=0.5, m=2.0, l_c=1/2, Fig. 15 shows the comparison of two cracked zones on the dynamic responses at the mid-span of the fourth span for the bridge. It can be seen that the maximal deflection of the beam with large crack zone is 1.24 times of that for the beam with small crack zone.

3.2.4 Effect of bridge surface roughness

The effects of the bridge roughness on the dynamic deflections are discussed in this section. As shown in Fig. 16, the vibration deflections at the mid-span of the fourth span for the bridge

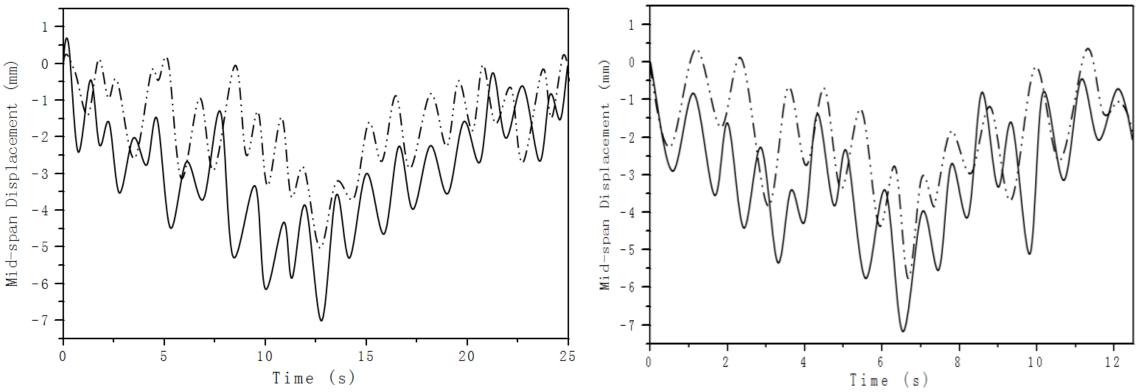

(a) Vehicle speed=40 km/h (b) Vehicle speed=80 km/h

Fig. 14 The comparison of the beam displacements with different number of cracked zones (——— Cracked beam with three cracked zones; — . . — Cracked beam with a cracked zone)

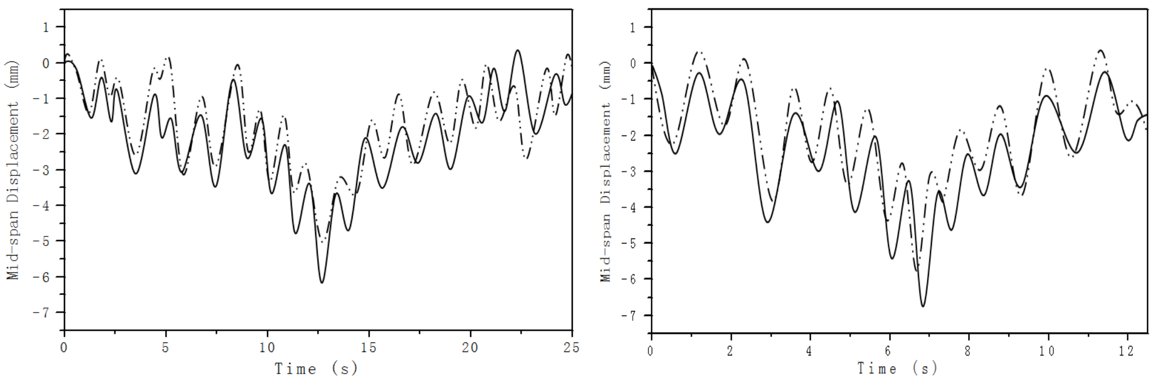

(a) Vehicle speed=40 km/h (b) Vehicle speed=80 km/h

Fig. 15 The comparison of two cracked zones on the dynamic responses (———large cracked zone; — . . — small cracked zones)

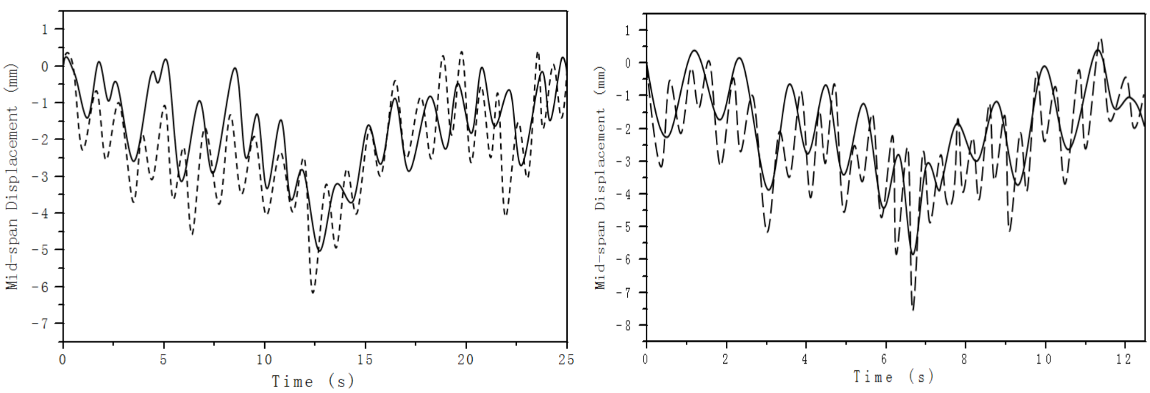

(a) Vehicle speed=40 km/h (b) Vehicle speed=80 km/h

Fig. 16 The comparison of the beam displacements under bridge surface roughness(———Tested roughness; -----Poor)

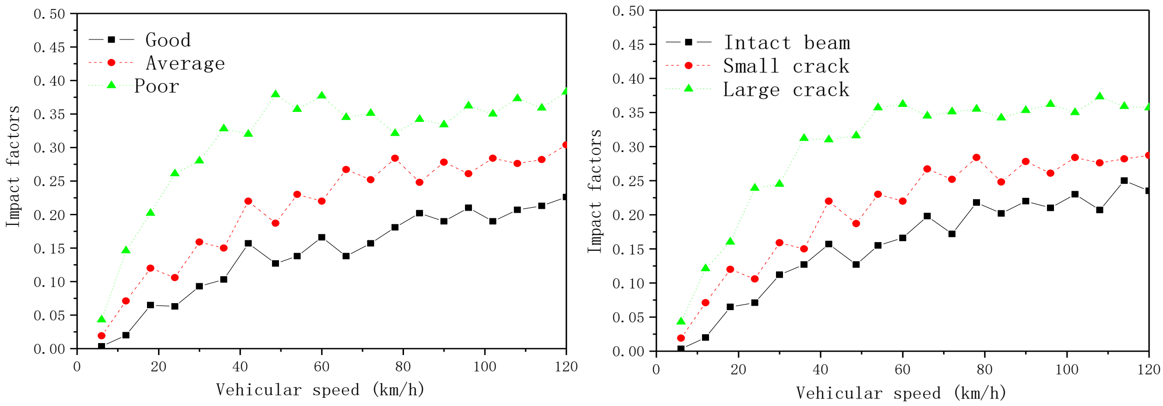

(a) Surface roughness (b) Crack parameters

Fig. 17 Impact factors of damaged beam

increase when the bridge roughness condition changes from tested roughness to Poor roughness. The maximum vertical deflections of the beam change from 5.0 mm to 6.13mm for tested roughness and poor roughness conditions. Therefore, the bridge surface condition has proven to have a large influence on the vibration of damaged bridges.

3.2.5 Impact factors of cracked beam

The impact factors of damaged beams are conducted under different vehicular speeds, three levels of bridge surface roughness, and two crack parameters. From Fig. 17, it is found that the impact factors increase significantly with the vehicular speed and bridge surface roughness increases. For example, for the damaged beam under the same vehicular speed of 60km/h, the impact factor increases from 0.17 for Good roughness to 0.38 for Poor roughness. For bridge surface with Average roughness, the effect of cracks on the impact factors is even more obvious, where the impact factors are equal to 0.22 and 0.36, respectively, corresponding to the small damaged beam and large damaged beam for the vehicle travel with 60km/h.

4. Conclusions

This study is mainly focused on establishing a new methodology which can fully consider the effect of the damaged bridge cracks, vehicle models, and bridge surface roughness conditions. Two vehicle models were introduced, including a four DOFs vehicle model and a full-scale vehicle model with seven DOFs. The bridges are modeled in two types, including a single-span uniform beam and a full scale reinforced concrete high-pier bridge, respectively. The crack zone in the reinforced concrete bridge is considered by a damage function. The bridge and vehicle coupled equations are established by combining the equations of motion of both the bridge and vehicles using the displacement relationship and interaction force relationship at the contact points.

The verifications of the numerical simulations demonstrated that:

• The proposed method can rationally simulate the vibration behaviors including the dynamic responses and impact factors of the damaged bridge under moving vehicles, and factors such as bridge surface roughness, bridge model, and crack parameters cannot affect the accuracy of the verifications;

• The crack is a key factor for the bridge dynamic responses of the vehicle-bridge coupled system, which can obviously increase the dynamic responses of bridge;

•For the bridge with no roughness, the effect of cracks on the impact factors is very small and can be neglected. For the bridge with roughness, however, the effect of cracks on the impact factors is very significant and cannot be neglected.

• The bridge surface condition has proven to have a large influence on the dynamic responses and impact factors of damaged bridges.

The successful application of the proposed methodology to simulate the dynamic response of a damaged bridge induced by the moving vehicles indicates that the proposed methodology can be applied to improve the current study of the interaction between bridges and vehicles. The proposed method will also be further developed to verify by the results tested by the real bridge structures in the future studies.

Acknowledgments

The authors gratefully acknowledge the financial support provided by the National Basic Research Program of China (973 Program) (Project No. 2015CB057702), the Natural Science Foundation of China (Project No.51108045), Theory Research and Engineering Application Team Innovation Project of Bridge Safety Control and Durability assessment (Project No. 15QLTD02), and Fund of Hunan Provincial Youth Talent (Project No. 2015RS4052).

References

Abdel Wahab, M.M., De Roeck, G. and Peeters, B. (1999), "Parameterization of damage in reinforced concrete structures using model updating", *J. Sound Vib.*, **228**(4), 717-730.

American Association of State Highway and Transportation Officials (AASHTO) (2004), LRFD bridge design specifications, Washington DC.

Ariaei, A., Ziaei-Rad, S. and Ghayour, M. (2009), "Vibration analysis of beams with open and breathing cracks subjected to moving masses", *J. Sound Vib.*, **326**, 709-724.

Chen, S.R. and Cai, C.S. (2004), "Accident assessment of vehicles on long-span bridges in windy environments", *J. Wind Eng. Ind. Aerodyn.*, **92**, 991-1024.

Chen, S.R. and Wu, J. (2010), "Dynamic performance simulation of long-span bridge under combined loads of stochastic traffic and wind", *J. Bridge Eng.*, **15**(3), 219-230.

Cheng, S.M., Wu, X.J. and Wallace, W. (1999), "Vibrational response of a beam with a breathing crack", *J. Sound Vib.*, **225**(1), 201-208.

Czaderski, C. and Motavalli, M. (2007), "40-Year-old full-scale concrete bridge girder strengthened with prestressed CFRP plates anchored using gradient method", *Compos. Part B: Eng.*, **38**, 878-886.

Deng, L. and Cai, C.S. (2010a), "Development of dynamic impact factor for performance evaluation of existing multi-girder concrete bridges", *Eng. Struct.*, **32**(1), 21-31.

Deng, L. and Cai, C.S. (2010b), "Identification of dynamic vehicular axle loads: Theory and simulations", *J. Vib. Control*, **16**, 2167-2194.

Deng, L. and Cai, C. S. (2011), "Identification of dynamic vehicular axle loads: demonstration by a field study", *J. Vib. Control*, **17**,183-195.

Dimarogonas, A.D. (1996), *Vibration Engineering*, St. Paul, Minnesota: West Publishers.
Dugush, Y.A. and Eisenberger, M. (2002), "Vibrations of non-uniform continuous beams under moving loads", *J. Sound Vib.*, **254**(5), 911-926.
Fryba, L. (1974), "Response of a beam to a rolling mass in the presence of adhesion", *Acta Technica CSAV*, **19**(6), 673-687.
Green, M.F. and Cebon, D. (1997), "Dynamic interaction between heavy vehicles and highway bridges", *Comput. Struct.*, **62**(2), 253-264.
Wang, T.L., Huang, D.Z. and Shahawy, M. (1992), "Dynamic response of multi-girder bridges", *J. Struct. Eng.*, **118**(8), 2222-2238.
Khoa, V.N. (2013), "Comparisons studies of open and breathing crack detections of a beam-like bridge subjected to a moving vehicle", *Eng. Struct.*. **51**, 306-314.
Law, S.S. and Zhu, X.Q. (2004), "Dynamic behavior of damaged concrete bridge structures under moving vehicular loads", *Eng. Struct.*, **261**, 279-293.
Law, S.S. and Zhu, X.Q. (2005), "Bridge dynamic responses due to road surface roughness and deceleration of vehicle", *J. Sound Vib.*, **282**(3-5), 805-830.
Lee, H.P. and Ng, T.Y. (1994), "Dynamic response of a cracked beam subject to a moving load", *Acta Mechanica*, **106**, 221-230.
Li, Q.S. (2002), "Free vibration analysis of non-uniform beam with an arbitrary number of cracks and concentrated masses", *J. Sound Vib.*, **252**(3), 509-525.
Mahmoud, M.A. and Abou Zaid, M.A. (2002), "Dynamic response of a beam with a crack subject to a moving mass", *J. Sound Vib.*, **256**(4), 591-603.
Neild, S.A., Williams, M.S. and McFadden, P.D. (2002), "Non-linear behavior of reinforced concrete beams under low amplitude cyclic and vibration loads", *Eng. Struct.*, **24**, 707-718.
Neild, S.A., Williams, M.S. and McFadden, P.D. (2003), "Nonlinear vibration characteristics of damaged concrete beams", *J. Struct. Eng.*, ASCE, **129**(2), 260-268.
Nguyen, K.V. and Tran, H.T. (2010), "A multi-cracks detection technique of a beam-like structure based on the on-vehicle vibration measurement and wavelet analysis", *J Sound Vib.*, **329**(21), 4455-4465.
Rizzo, P. and Scalea, F.L. (2006), "Feature extraction for defect detection in strands by guided ultrasonic waves", *Struct. Health Monit.*, **5**(3), 297-308.
Shifrin, E.I. and Ruotolo, R. (1999), "Natural frequencies of a beam with an arbitrary number of cracks", *J. Sound Vib.*, **222**, 409-423.
Yang, Y.B., Yau, J.D. and Wu, Y.S. (2004), *Vehicle-bridge interaction dynamics with applications to high speed railways*, World Scientific, Singapore.
Yin, X.F., Fang, Z., Cai, C.S. and Deng, L. (2010), "Non-stationary random vibration of bridges under vehicles with variable speed", *Eng. Struct.*, **32**(8), 2166-2174.
Yin, X.F., Fang, Z. and Cai, C.S. (2011), "Lateral vibration of high-pier bridges under moving vehicular loads", *J. Bridge Eng.*, **16**(3), 400-412.
Zhang, W. and Cai, C.S. (2012), "Fatigue reliability assessment for existing bridges considering vehicle speed and road surface conditions", *J. Bridge Eng.*, **17**(3), 443-453.

CC